Metallophysics and Advanced Technologies
Металофіз. новітні технол.
Metallofiz. Noveishie Tekhnol.
2026, vol. 48, No. 8, pp. 827–841
https://doi.org/10.15407/mfint.48.08.0827
Reprints available directly from the publisher

© 2026 G. V. Kurdyumov Institute for Metal Physics,
National Academy of Sciences of Ukraine
Published by license under
the G. V. Kurdyumov Institute for Metal Physics–
N.A.S. of Ukraine Publishers imprint.
Printed in Ukraine.

PACS numbers: 61.72.Ff, 62.20.Qp, 68.35.Ct, 68.70.+w, 81.40.Wx, 81.65.Ps, 83.60.Np

Magnetic Post-Processing of Additively-Manufactured Inconel 718 Superalloy: Functional Microrelief Evolution and Surface Strain Hardening

D. A. Lesyk[*,**,***], B. M. Mordyuk[***], O. Stamann[****], D. Grochala[*****], S. S. Salii[**], M. M. Lytvynenko[**], M. V. Romanenko[**], M. I. Anyakin[**], A. Lamikiz[*]

[*]*National Technical University of Ukraine 'Igor Sikorsky Kyiv Polytechnic Institute', 37 Beresteiskyi Prosp., UA-03056 Kyiv, Ukraine*
[**]*University of the Basque Country, Barrio de Sarriena, s/n, SP-48940 Leioa, Spain*
[***]*G. V. Kurdyumov Institute for Metal Physics, N.A.S. of Ukraine, 36 Academician Vernadsky Blvd., UA-03142 Kyiv, Ukraine*
[****]*Otto-von-Guericke University Magdeburg, 2 Universitätsplatz, DE-39106 Magdeburg, Germany*
[*****]*West Pomeranian University of Technology, 17 al. Piastyw, PL-70-310 Szczecin, Poland*

Nickel-based superalloys with enhanced operational properties are key materials for producing safety-critical components. Additive manufacturing offers a new way to manufacture critical components, enabling the production of superalloy structures with complex shapes, which are unattainable by con-

Corresponding author: Bohdan Mykolayovych Mordyuk
E-mail: mordyuk@imp.kiev.ua

Citation: D. A. Lesyk, B. M. Mordyuk, O. Stamann, D. Grochala, S. S. Salii, M. M. Lytvynenko, M. V. Romanenko, M. I. Anyakin, and A. Lamikiz, Magnetic Post-Processing of Additively-Manufactured Inconel 718 Superalloy: Functional Microrelief Evolution and Surface Strain Hardening, *Metallofiz. Noveishie Tekhnol.*, **48**, No. 8: 827–841 (2026), DOI: 10.15407/mfint.48.08.0827

© Publisher PH 'Akademperiodyka' of the NAS of Ukraine, 2026. This is an open access article under the CC BY-ND license (https://creativecommons.org/licenses/by-nd/4.0)

ventional manufacturing methods. The laser powder bed fusion (LPBF) process is used for manufacturing superalloy components. Post-processing methods are required to improve the surface integrity, because LPBF parts with complex geometries suffer from various defects located both on the surface and near-surface layers. Today, post-processing methods are being developed to improve surface integrity in LPBF-produced parts. In this work, magnetic needle finishing (MNF) is applied for surface post-processing of Inconel 718 superalloy manufactured *via* LPBF. The effects of magnetic needle finishing under optimised conditions on surface morphology, functional relief performance, microstructure, and hardness are investigated. The results indicate that the surface integrity of the LPBF-manufactured 718 alloy is improved by generating a smoothed surface microrelief with a strain-hardened subsurface layer (the macrohardness increased from $\cong 32\ HRC_{10}$ to $\cong 39\ HRC_{10}$) through the high-energy MNF post-processing. Reducing and levelling the amplitude parameters (the R_a parameter is decreased from $\cong 4.0$ μm to $\cong 2.0$ μm) of microirregularities in the MNF-finished Inconel-alloy samples due to the multiple-angle impact of magnetic pins resulted in a redistribution of surface load, which is favourable for the functional performance of the LPBF-produced parts. A decrease in crystallite size as well as an increase in lattice strain and dislocation density due to the surface plastic deformation of the near-surface layer are confirmed.

Key words: magnetic finishing, Inconel 718, laser powder bed fusion, post-processing, surface integrity, functional relief performance, microstructure.

Ніклеві суперстопи з поліпшеними експлуатаційними властивостями є ключовими матеріялами для виробництва критично важливих деталів, від яких залежить безпека. Адитивне виробництво відкриває новий спосіб виготовлення відповідальних деталів, уможливлюючи одержання конструкцій із суперстопів складної форми, створення яких є неможливим класичними методами оброблення. Для виготовлення деталів із суперстопів застосовується процес лазерного пошарового стоплення порошку (ЛПСП). Однак вироби складної геометрії, виготовлені методою ЛПСП, мають різноманітні дефекти, розташовані як безпосередньо на поверхні, так і в приповерхневих шарах, що зумовлює необхідність застосування методів постоброблення для поліпшення цілісности поверхні. Сьогодні активно розробляються нові методи поверхневого фінішного оброблення деталів, виготовлених методою ЛПСП. У цій роботі для фінішного постоброблення поверхні суперстопу Інконель 718, виготовленого методою ЛПСП, було застосовано магнетне фінішне оброблення (МФО). Досліджено вплив МФО за оптимізованих режимів на морфологію поверхні, функціональні характеристики рельєфу, мікроструктуру та твердість. Результати свідчать, що цілісність поверхні виробленого за ЛПСП-технологією стопу 718 було поліпшено за рахунок формування згладженого мікрорельєфу поверхні та деформаційного зміцнення поверхневого шару (макротвердість збільшилася від $\cong 32\ HRC_{10}$ до $\cong 39\ HRC_{10}$) під дією високоенергетичного МФО. Зменшення та вирівнювання амплітудних параметрів мікронеоднорідностей (параметер R_a зменшився від $\cong 4{,}0$ мкм до $\cong 2{,}0$ мкм) у зразках стопу Інконель 718 після МФО внаслідок багатовекторного ударного впливу магнетних штифтів привели до перерозподілу поверх-

невого навантаження, що є сприятливим чинником для функціональних характеристик ЛПСП-деталів. Унаслідок поверхневої пластичної деформації підтверджено зменшення розміру кристалітів і збільшення деформації ґратниці та густини дислокацій у поверхневому шарі.

Ключові слова: магнетне фінішне оброблення, Інконель 718, лазерне пошарове стоплення порошку, постоброблення, поверхнева цілісність, функціональні характеристики рельєфу, мікроструктура.

(Received July 09, 2026; in final version, September 08, 2026)

1. INTRODUCTION

Laser powder bed fusion (LPBF) technology is one of the advanced additive manufacturing methods for producing complexly shaped nickel-based superalloy components [1, 2]. The metal powder layer of a certain thickness is selectively melted *via* a moving laser beam, generating a layered 3*D* object. As compared to the LPBF process [1, 3–5], an overblown metal powder or metal wire at the direct energy deposition process is placed in a specific place and melted by means of a high-energy laser beam [6–8]. The advanced LPBF 3D printing process offers a new alternative way for manufacturing small-size metallic components with complex geometries. The LPBF technology is a very valuable approach for additive manufacturing heat-resistant alloy (Inconel) products [1, 3, 9–12].

Surface integrity improvement in the nickel-based superalloy parts produced by the LPBF technique is a crucial issue in the additive manufacturing routes. On the one hand, the application of specific heat post-treatments needs to eliminate microstructural anisotropy, improving the mechanical properties [10, 13–15]. On the other hand, surface modification treatments should be applied in combination with thermal post-treatments to improve the surface and structural integrity in nickel-based superalloys [4, 10, 14, 15–17]. Currently, various conventional mechanical and chemical surface post-treatment methods are applied to reduce the surface roughness and enhance the mechanical properties of Inconel alloys. Barrel/vibratory finishing [18, 19] and abrasive finishing [4, 10, 20–22] have been used for the surface post-processing of additively manufactured metal parts. The use of laser polishing is another non-abrasive approach for the significant improvement of surface roughness [23]. Laser shock peening [17, 24], cavitation peening [25], and ultrasonic-based surface finishing [14, 17, 26–29] were also applied, aiming to induce nanostructuring and compressive stresses. The mechanical surface post-treatment by ultrasonic tools is one of the most effective approaches to enhance the surface integrity and properties in the near-surface layers of 3*D*-produced Ni-based alloy parts. At the same time, ultrasonic methods are limited for

surface finishing of complexly shaped and/or small-size geometries compared to abrasive finishing methods. Magnetic-assisted surface finishing, chemical and electrochemical surface modification (polishing) are more flexible processes, which are applied for post-treatment of metal parts with complex geometries manufactured *via* LPBF.

Nowadays, magnetically driven surface finishing methods are considered to improve the surface integrity of the nickel-based superalloy components with complex geometries manufactured through LPBF [16, 30]. During the magnetic abrasive finishing of the LPBF components, the material is uniformly removed from both the external and internal surfaces, eliminating the partially melted powder particles and smoothing the surface (R_a decreased from $\cong 7$ μm to less than 1 μm [31]. Magnetic abrasive finishing combined with vibratory machining significantly reduced the surface roughness (R_a values from 1.21 μm to 0.8 μm under optimal conditions) of the LPBF-fused Inconel 939 components [32]. In work [33], magnetic abrasive finishing was applied for the surface post-processing of the heat-treated Inconel 718 alloy manufactured by LPBF, mainly introducing high-angle grain boundaries and subsequently improving mechanical properties.

Unlike traditional magnetic abrasive finishing, magnetic needle finishing (MNF) uses magnetically driven ferromagnetic needles to induce micropeening alongside surface smoothing. In the MNF process, the material surface undergoes moderate plastic deformation under the high-speed impact of magnetic needles, uniformly distributing impact dimples on the surface [30]. At the same time, attempts to use magnetic needle finishing improving the surface integrity of the nickel-based superalloy parts manufactured by LPBF are practically absent. This research work examines the effect of wet magnetic needle finishing on the functional microrelief, the surface roughness, microstructure and internal defects in the Inconel 718 superalloy parts manufactured by the LPBF additive manufacturing method.

2. EXPERIMENTAL DETAILS

2.1. Powder Material and LPBF Method Description

For post-processing, Inconel 718 (IN718) alloy samples were manufactured using the RENISHAW AM400 machine and a commercial nickel-based pre-alloyed IN718 metal powder (the nominal chemical composition [wt.%] is the following: 50–55% Ni, 17–21% Cr, 4.7–5.5% Nb, 2.8–3.3% Mo, 0.6–1.2% Ti, and 0.2–0.8% Al) with high quality. The powder used contained spherical powder particles in the range of 10–55 μm. IN718 alloy parts were manufactured by LPBF using a layer thickness of 60 μm. The key parameters for manufacturing IN718 alloy parts were a laser power of 200 W and a scanning speed of 700 mm/s, using a

multidirectional scanning strategy with a stripe spacing of 5 mm.

2.2. Post-Processing Method Description

Surface post-processing of the LPBF-manufactured IN718 alloy samples was implemented using a magnetically driven magnetic needle finishing (MNF) method. The MNF post-processing of the LPBF-manufactured small-size parts was conducted under a variable magnetic field using a multicomponent media, consisting of ferromagnetic needles and an abrasive paste enriched with surface-active substances, lowered into a chamber [16]. The MNF system comprised a cylindrical processing chamber with liquid compound, a magnetic disk drive, and an electric motor. The MNF process was performed for 30 min at room temperature.

2.3. Experimental Methods Description

The surface samples before and after post-processing were observed by a Mitutoyo Hyper Quick Vision WLI 3D optical profilometer (ISO 25178-2:2012 and ISO 21920-2:2021 standards) and 3D Taylor Hobson Form Talysurf 120 contact profilometer (ISO 4287:1997 and ISO 21920-2:2021 standards). The bearing area parameters (S_{pk}, S_k, S_{vk}) and functional volume parameters (V_{mc}, V_{mp}, V_{vc}, V_{vv}) obtained from the surface (0.5 mm by 0.5 mm area) were analysed. The profile roughness (R_a, R_p, R_v, R_t) parameters along the 0.8 mm sampling length were also examined in this study.

The microstructure and bulk/surface defects in the build and scan direction cross-sections of the LPBF-manufactured and MNF-processed samples were observed by the Leica MEF4A and Polyvar 2 light optical microscopes (LOM), and the high-resolution TESCAN Mira 3 LMU scanning electron microscope (SEM).

X-ray diffraction (XRD) analysis was performed using a Rigaku Ultima IV diffractometer. The quantitative analysis of residual internal defects was statistically carried out using the cross-sectional optical (unetched) micrographs obtained from the build direction by means of the Image-Pro Plus software through grayscale threshold segmentation. Macrohardness measurements were performed on the unpolished outer surfaces using a DIA-TESTOR 2Rc Rockwell hardness tester under an indenter load of 10 kgf.

3. RESULTS AND DISCUSSION

The surface topography, functional microrelief parameters, and roughness alterations are studied in the first part of this study (Figs.

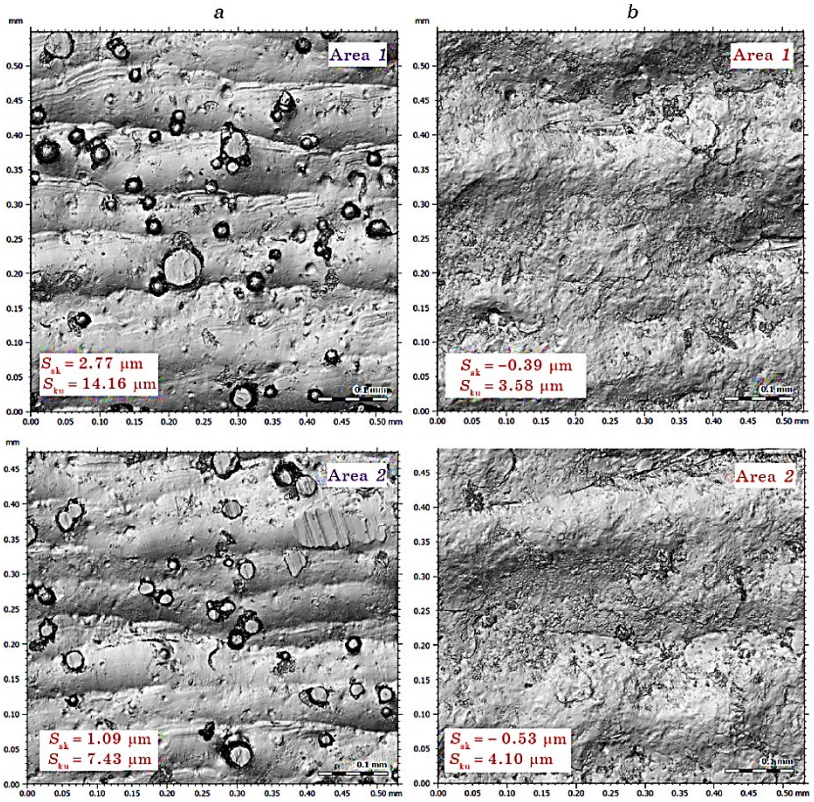


Fig. 1. Surface morphology and height distribution (S_{sk} and S_{ku}) parameters of the LPBF-manufactured (*a*) and MNF-finished (*b*) alloy IN718 samples across Area *1* and Area *2*.

1–3), while the structural–phase state and strain-hardened effect are observed in the second part of this work (Figs. 4–6), clarifying the surface integrity in the IN718 alloy specimens manufactured by LPBF and subsequently post-processed by MNF.

3.1. Surface Microrelief and Morphology

The surface microreliefs/morphologies (Fig. 1), functional bearing capacity (Fig. 2) and material volume parameters of the laser powder bed fused and magnetic needle finished alloy IN718 samples were examined across two representative sample regions (Area *1* and Area *2*) and compared. The MNF process resulted in the removal of partially adhered spherical powder particles due to surface plastic deformation with multiangle collisions of needles, smoothing ($\downarrow S_a$ parameter) and flattening ($\downarrow\downarrow S_p$ parameter) the surface. The MNF finishing slightly

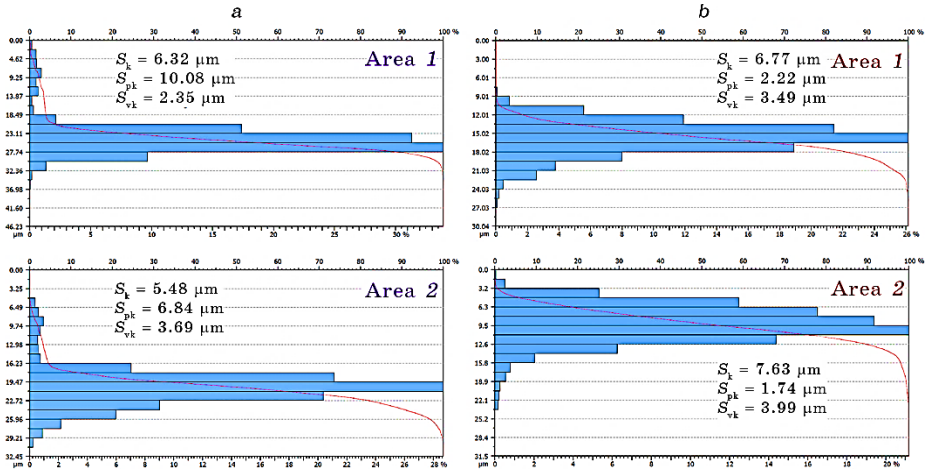


Fig. 2. Load-bearing (S_k, S_{pk}, and S_{vk}) parameters derived from Abbott–Firestone curves for the LPBF-manufactured (*a*) and MNF-finished (*b*) alloy IN718 samples across Area *1* and Area *2*.

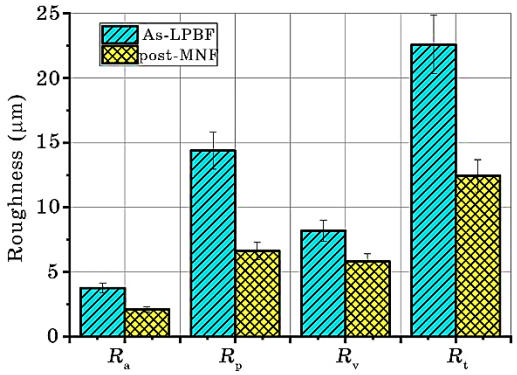


Fig. 3. Surface roughness of the LPBF-manufactured and MNF-finished superalloy IN718 samples.

reduced the arithmetical mean height (S_a = 1.95 μm, 15%-reduction compared to the LPBF sample) parameter, while the maximum peak height (S_p) parameter significantly decreased (from 20–25 μm to 10–15 μm). The maximum valley height (S_v) values in the as-LPBF and post-MNF samples are at the same level, confirming a negligible effect of the high-speed needle impacts on the valley surface.

As illustrated in the topographic images (Fig. 1) of the measured area (500 μm×500 μm), the boundaries of laser tracks were smoothed but not completely removed/erased from the surface because the nickel-based surface samples were subjected to moderate MT conditions.

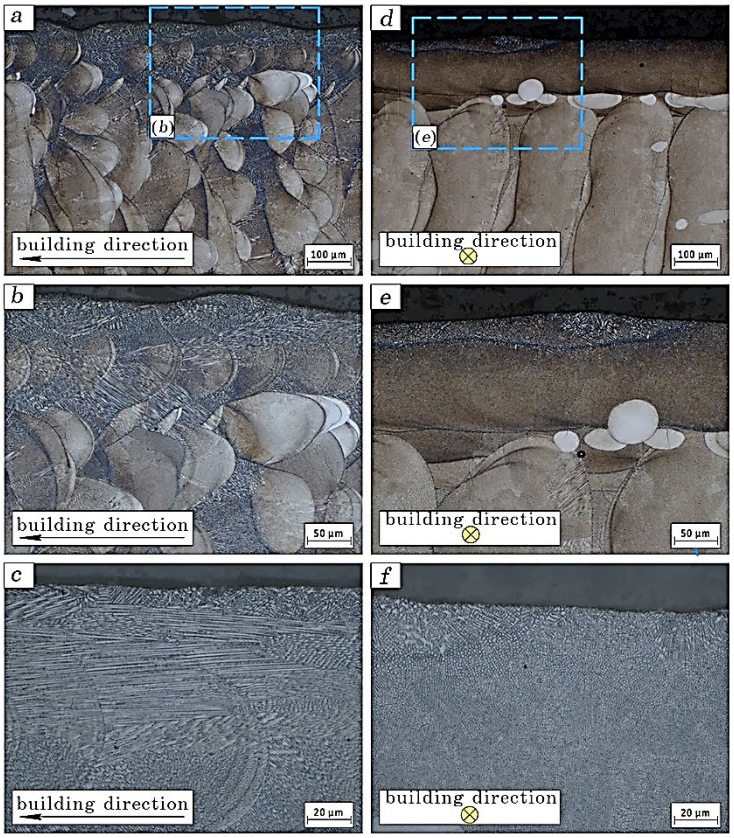


Fig. 4. Macrostructure and microstructure of the LPBF-manufactured (*a*) and MNF-finished (*b*) alloy IN718 samples in the build (*a*–*c*) and scan (*d*–*f*) directions.

Thus, a flattened and wavy surface microrelief with a uniformly distributed dimpled texture (Fig. 1, *b*) due to the individual needle impacts and traces of laser tracks is formed after magnetically driven surface post-processing.

Comparative 2*D* surface morphologies and height distribution (S_{sk} and S_{ku}) parameters that reflect the degree of roughness profile shift, evaluated in the LPBF additive manufacturing conditions (Fig. 1, left) and MNF post-processing conditions (Fig. 1, right), demonstrate that the skewness values are a pronounced positive asymmetry ($S_{sk} > 0$: +2.77 in Area *1* and +1.09 in Area *2*) across both areas in the as-LPBF conditions due to the presence of adhered powder particles and sharp peaks.

Conversely, application of magnetic post-processing using numerous and repetitive pin impacts resulted in negative near-Gaussian skewness values across both areas ($S_{sk} < 0$: –0.39 in Area *1* and –0.53 in

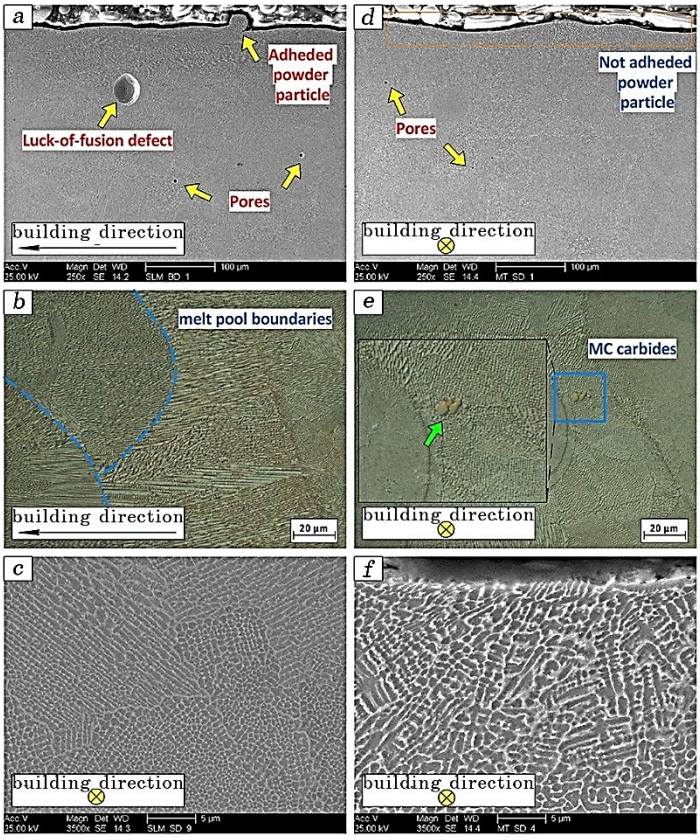


Fig. 5. Microstructure observation by SEM and LOM in the LPBF-manufactured (*a*–*c*) and MNF-finished (*d*–*e*) alloy IN718 samples in the build and scan directions.

Area *2*), which is a relief with a predominance of valleys over peak. The kurtosis (S_{ku}) values that represent the degree of the roughness profile sharpness decreased from 14.16 / 7.43 to 3.58 / 4.10 after the MNF treatment, indicating the elimination of high peaks and the formation of a uniformly smoothed surface texture.

3.2. Functional Microrelief Performance

The functional bearing ratio values and volume parameters with the minimised S_{pk}/V_{mp}, expanded core S_k/V_{mc}, and moderate S_{vk}/V_{vv} alterations demonstrate that the generated surface in the MNF-treated samples possesses the ability to suppress the initial wear during running-in ($\downarrow\downarrow S_{pk}$) and increase the load-bearing capacity due to an increase in the area of actual contact ($\uparrow S_k$) (Fig. 2).

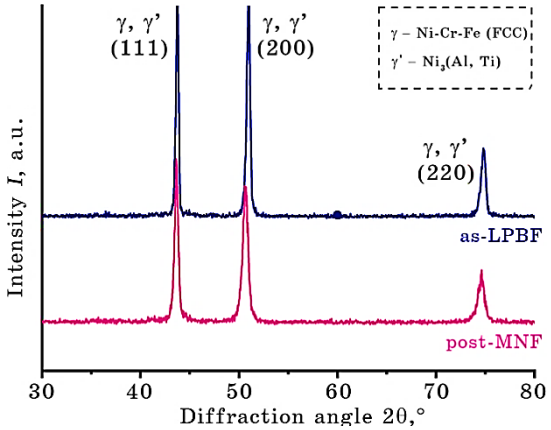


Fig. 6. XRD phase patterns for the LPBF-manufactured and MNF-finished alloy IN718 samples.

In addition, the depth of the valleys does not decrease, but rather increases slightly or remains stable (2.35 μm to 3.49 μm in Area *1* and 3.69 μm to 3.99 μm in Area *2*), confirming that the MNF process deforms the surface locally. The metal pins with multiple microimpacts rotated at high-speed remove high peaks selectively without filling or destroying the intertrack valleys that can create the condition of the microreservoirs to retain lubricant (V_{vv} from 0.0025 mm^3/mm^2 to 0.0036 mm^3/mm^2 in Area *1*).

The surface profile roughness (R_a, R_p, R_v, and R_t) parameters (Fig. 3), estimated from their profiles along the 0.8 mm sampling length, indicate that the magnetically driven surface finishing treatment resulted in a reduction in the surface roughness, correlating well with the area surface roughness. The surface roughness (R_a) parameter was reduced from ≅3.7 μm to ≅2.10 μm after the surface MT post-processing, confirming a significant effect on surface quality improvement. It can be seen that a dramatic reduction in peak height (R_p) was achieved, dropping by over 50% (from ≅14.5 μm to ≅6.5 μm), indicating effective removal of high-peak microasperities in the IN718 alloy through the MT finishing process.

Reducing and levelling the amplitude parameters of micro-irregularities in the MNF-finished Inconel alloy samples due to the high-speed impact of magnetic pins with various collisions leads to a redistribution of surface load, which is favourable for the functional performance of the LPBF-produced parts in extreme conditions. The high-speed needle impacts on the surface ensure micropeening and plastic flattening, rather than just removal of the partially melted/adhered powder particles from the surface. Thus, surface post-processing using the magnetic needle finishing transforms the original

rough and wavy-shaped surface into a smoothed and flattened surface microrelief with a uniformly distributed dimpled texture, resulting in improved surface integrity of Inconel 718 alloy prepared *via* LPBF.

3.3. Microstructure

To examine the near-surface structure, phase composition, and internal/surface defects in as-LPBF IN718 alloy before and after the MT finishing, light optical microscopy, scanning electron microscopy, and x-ray diffraction methods were applied in this study. The macrostructure and microstructure of the LPBF-manufactured and MNF-finished alloy IN718 samples in the build (Fig. 4, *a*–*c*) and scan (Fig. 4, *d*–*f*) directions are presented in Fig. 4 and Fig. 5.

Micrographs of the microstructure of the LPBF-manufactured and surface post-processed IN718 alloy specimens obtained using LOM (Figs. 4 and 5) and SEM (Fig. 5) with high-magnification along build and scan directions demonstrated that the dendritic structure, containing γ [Ni–Cr–Fe] solid solution matrix with a face-centred cubic (f.c.c.) lattice, mainly consists of elongated colonies of cells in the build direction (Fig. 4, *a*–*c*, Fig. 5, *a*, Fig. 5, *b*), oriented parallel to the primary thermal gradient during solidification, while the equiaxed cellular colonies of finely dispersed cells are observed in the scan direction (Fig. 4, *d*–*e*, Fig. 5, *c*–*f*).

The microsegregation of some alloying elements, such as niobium (Nb), molybdenum (Mo), and carbon (C) corresponds to interdendritic Laves phase and carbides (MC) (Fig. 5, *e*), which are uniformly distributed within the intercellular regions [2, 22, 34, 35]. The LPBF-built IN718 alloy specimens with a dendritic structure were characterised by increased macrohardness ($\cong 32\ HRC_{10}$). Finishing by MNF increased the surface macrohardness by $\cong 20\%$ ($\cong 39\ HRC_{10}$) owing to numerous and repetitive pin impacts, which promote near-surface plastic deformation resulting from micropeening and sliding.

Notably, based on the SEM micrographs (Fig. 5, *f*), the dendritic cells were revealed to be precisely located at the subsurface edge of the MNF-processed samples, confirming the lack of interfacial delamination, severe plastic folding or microcracking during the removal of irregularities/peaks on the LPBF-formed surface. This confirms that the numerous dynamic impacts of the metallic needles under the action of an alternating magnetic field promote a controlled removal of metal with the MNF process, in which localised work hardening is generated. Additionally, as seen in Fig. 5, *a* (as-LPBF) and Fig. 5, *b* (post-MNF), compared to the as-built IN718 alloy specimen [31], partially melted powder particles and/or adhered spherical/ellipsoidal balls were removed/reduced from the surface by the MNF finishing.

As noted above, the microstructure comprises the dendritic struc-

ture regardless of the studied condition (as-LPBF and post-MNF), containing γ [Ni–Cr–Fe] solid solution matrix with a face-centred cubic (f.c.c.) lattice, γ' [Ni_3(Al, Ti)], Laves phases [$(Ni, Fe, Cr)_2$(Nb, Mo, Ti)], and MC carbides [(Ti, Nb)C], which are identified in the initial as-LPBF condition (Fig. 6). Primary strengthening elements (such as Nb) remain largely segregated within interdendritic Laves phases and MC carbides and/or trapped in the solid solution matrix due to the extremely high cooling rates in the LPBF process.

The observed XRD patterns show a clear shift of the γ/γ' diffraction peaks toward smaller 2θ-angles after the MNF post-processing (Fig. 6), which is in strong agreement with previously published studies on surface mechanical treatment *via* severe plastic deformation of the Inconel 718 manufactured *via* LPBF [19, 36]. The (220) peak shift (Fig. 6) corresponds to lattice expansion along the normal surface, confirming the induction of beneficial residual compressive macrostresses (≅ 1 GPa) in the subsurface layer instead of the manufacturing induced tensile stresses. Additionally, the moderate broadening of the γ/γ' diffraction (220) peaks aligns with the reduction in crystallite size and the increase in lattice strain (0.32%), providing clear evidence of notable near-surface plastic deformation and dislocation accumulation ($2.41 \cdot 10^{-14}$ m^{-2}) in the parts subjected to the magnetic needle finishing process.

Thus, magnetic needle finishing is an effective method for surface post-processing of IN718 alloy parts manufactured *via* the LPBF technique. In Refs. [37, 38], it was shown that MNF treatment under a spatial composite magnetic field can significantly extend the processing range, increase the effective processing area height by 200%, and improve the uniformity of the workpiece surface morphology. The high-quality MNF finishing is attributed to microcutting material removal, surface smoothing through sliding, and surface hardening *via* micropeening. Compared to barrel finishing [39–41], which is used for the surface post-processing of complexly shaped metal components, magnetic needle finishing is a flexible post-processing method for the LPBF-manufactured small-scale components.

4. CONCLUSION

The current study demonstrated that the high-quality magnetic needle finishing (MNF process applied for surface post-processing of Inconel 718 alloy parts improved surface quality and microstructural characteristics. The surface integrity of the LPBF-manufactured nickel-based superalloy was improved by generating a smoothed surface microrelief with a strain-hardened subsurface layer, creating a synergistic effect of hardening and finishing simultaneously.

The results indicate that the magnetic needle finishing (MNF) flattened surface irregularities (R_p parameter decreased from ≅ 14.5 μm to

$\cong 6.5$ μm) and improved surface finish consistency, eliminating partially melted and adhered powder particles from the surface due to the high-speed impact of magnetic pins with different surface collisions, which promotes near-surface plastic deformation and surface smoothing (R_a decreased from $\cong 4.0$ μm to $\cong 2.0$ μm).

The functional parameters show that the formed surface reliefs in the MNF-treated samples possess the ability to suppress the initial wear during running-in ($\downarrow\downarrow S_{pk}$) and increase the load-bearing capacity due to an increase in the area of actual contact ($\uparrow S_k$).

The observed surface hardening (increased *HRC* value from $\cong 32$ HRC_{10} to $\cong 39$ HRC_{10}) and high lattice microstrain measured by XRD is attributed to the increased dislocation density and grain refinement within the fine dendritic structure of the MNF-processed near-surface layer of the IN718 alloy specimens. In addition, the XRD data confirmed formation of residual compressive macrostresses after applying the MT finishing.

ACKNOWLEDGEMENT

The authors gratefully acknowledge the support of the European Union's HORIZON 2020 Research and Innovation Programme under the Marie Sklodowska-Curie Grant (agreement No. 101034379) and the National Research Foundation of Ukraine under the Science for the Recovery of Ukraine in the War and Post-War Periods Grant (agreement No. 2022.01/0038). The work was also partially supported by the German Academic Exchange Service (DAAD) under the Research Grants for Doctoral Candidates and Young Academics and Scientists program. The authors would like to thank retired professor V. V. Dzhemelinskyi (Igor Sikorsky Kyiv Polytechnic Institute, Ukraine) and Dr. S. Martinez (University of the Basque Country) for the support provided with the MNF-post-processing tests and LPBF-manufacturing samples, respectively. Additionally, the authors would like to thank S. Faust (Otto von Guericke University Magdeburg, Germany) for the support provided with the surface roughness measurements.

AUTHORS' CONTRIBUTIONS

D.A.L. planned this research, performed the MNF experiments, analysed the experimental data, prepared the graphic material, and wrote the manuscript with input from all authors. B.M.M. collected data on integrity properties of Inconel alloys manufactured by LPBF, analysed the XRD data and took part in the preparation of the article text. O.S. reviewed the literature and collected data on advanced mechanical surface post-processing methods, obtained the surface roughness data and

analysed the functional relief performance parameters. D.G. obtained the surface topography data and analysed the functional relief performance parameters. S.S.S. reviewed the literature and collected data on advanced additive manufacturing methods and interpreted the data. M.M.L. prepared the samples for LOM and SEM observations. M.V.R. prepared the samples for LOM and SEM observations. M.I.A. discussed the results obtained. A.L. took part in the preparation of the article text and discussed the results obtained.

REFERENCES

1. G. M. Volpato, U. Tetzlaff, and M. C. Fredel, *Addit. Manuf.*, **55**: 102871 (2022).
2. A. Vafadar, F. Guzzomi, A. Rassau, and K. Hayward, *Appl. Sci.*, **11**: 103729 (2021).
3. K. Li, J. Zhan, Y. Wang, Y. Qin, N. Gong, D. Z. Zhang, S. Tan, L. E. Murr, and Z. Liu, *J. Manuf. Process.*, **133**: 285 (2025).
4. D. A. Lesyk, S. Martinez, A. Lamikiz, O. O. Pedash, and B. N. Mordyuk, *Advanced Manufacturing Processes VI. Lect. Notes Mech. Eng.* (Eds. V. Tonkonogyi *et al.*) (Cham: Springer: 2025).
5. F. Venturi and R. Taylor, *J. Mater. Eng. Perform.*, **32**: 6589 (2023).
6. R. Zhuk, Z. Chen, M. Anyakin, and J. Yao, *Int. J. Adv. Manuf. Technol.*, **108**: 1163 (2020).
7. V. Kovalenko, J. Yao, Q. Zhang, M. Anyakin, X. Hu, and R. Zhuk, *Procedia CIRP*, **42**: 96 (2016).
8. M. Sokolovskyi, O. Siora, Y. Yurchenko, V. Lukashenko, D. Harder, L. Nyrkova, S. Osadchuk, and A. Bernatskyi, *Defect Diffus. Forum*, **448**: 61 (2026).
9. P. Gradl, D. C. Tinker, A. Park, O. R. Mireles, M. Garcia, R. Wilkerson, and C. Mckinney, *J. Mater. Eng. Perform.*, **31**: 6013 (2022).
10. D. A. Lesyk, B. N. Mordyuk, S. Martinez, O. O. Pedash, and A. Lamikiz, *Advanced Manufacturing Processes VI. Lect. Notes Mech. Eng.* (Eds. V. Tonkonogyi *et al.*) (Cham: Springer: 2026).
11. T. Thuneman, K. S. Raja, and I. Charit, *Crystals*, **14**: 89 (2024).
12. D. A. Lesyk, S. Martinez, and A. Lamikiz, *Procedia CIRP*, **124**: 89 (2024).
13. S. Ozer, M. A. Yalçın, G. M. Bilgin, K. Davut, Z. Esen, and A. F. Dericioglu, *J. Alloys Compd.*, **1012**: 178465 (2025).
14. D. A. Lesyk, S. Martinez, V. V. Dzhemelinskyi, O. Stamann, B. N. Mordyuk, and A. Lamikiz, *Advances in Design, Simulation and Manufacturing III. Lect. Notes Mech. Eng.* (Eds. V. Ivanov *et al.*) (Cham: Springer: 2020).
15. D. A. Lesyk, S. Martinez, B. N. Mordyuk, V. V. Dzhemelinskyi, and A. Lamikiz, *Advances in Design, Simulation and Manufacturing VII. Lect. Notes Mech. Eng.* (Eds. V. Ivanov *et al.*) (Cham: Springer: 2024).
16. D. A. Lesyk, S. Martinez, V. V. Dzhemelinskyi, O. Stamann, B. N. Mordyuk, and A. Lamikiz, *Proc. 2020 IEEE 10th Int. Conf. Nanomaterials: Applications & Properties (NAP)* (Sumy: 2020), p. 02SAMA17-1.
17. D. A. Lesyk, A. M. Ralls, B. N. Mordyuk, P. L. Menezes, I. Charit, and A. Lamikiz, *New Technologies, Development and Application VIII. Lect. Notes Networks Syst.* (Eds. I. Karabegović *et al.*) (Cham: Springer: 2025), vol. **1482**, p. 145.
18. A. Boschetto, L. Bottini, L. Macera, and F. Veniali, *Appl. Sci.*, **10**: 138 (2020).

19. D. A. Lesyk, B. N. Mordyuk, S. Martinez, V. V. Dzhemelinskyi, D. Grochala, A. V. Kotko, and A. Lamikiz, *Coatings*, **15**, Iss. 4: 425 (2025).
20. D. A. Lesyk, V. V. Dzhemelinskyi, S. Martinez, D. Grzesiak, and B. N. Mordyuk, *Advanced Manufacturing Processes IV. Lect. Notes Mech. Eng.* (Eds. V. Tonkonogyi *et al.*) (Cham: Springer: 2023).
21. C. S. Bagherifard, N. Beretta, S. Monti, M. Riccio, M. Bandini, and M. Guagliano, *Mater. Des.*, **145**: 28 (2018).
22. D. A. Lesyk, B. N. Mordyuk, S. Martinez, V. V. Dzhemelinskyi, D. Grzesiak, D. Grochala, and A. Lamikiz, *Lasers Manuf. Mater. Process.*, **10**: 702 (2023).
23. L. Beránek, V. Rana, Z. Pitrmuc, S. Pathak, L. Pelikán, Š. Petrášek, L. Hlavůňková, P. Zeman, A. Čermák, J. Kopeček, J. Resl, J. Steklý, O. Gregor, P. Novák, and M. Maštera, *J. Mater. Res. Technol.*, **43**: 2672 (2026).
24. J. A. Banderas-Hernández, C. Rubio-González, and A. Gómez-Ortega, *Int. J. Adv. Manuf. Technol.*, **132**: 669 (2024).
25. H. Soyama, D. Eakins, and A. M. Korsunsky, *Int. J. Fatigue*, **203**: 109342 (2026).
26. L. Chen, J. Xie, Y. Li, G. Yu, X. Zhang, and X. Ren, *J. Mater. Res. Technol.*, **33**: 7668 (2024).
27. D. A. Lesyk, S. Martinez, B. N. Mordyuk, O. O. Pedash, V. V. Dzhemelinskyi, and A. Lamikiz, *Post-Processing Techniques for Additive Manufacturing* (Eds. Z. Alam, F. Iqbal, and D. A. Khan) (Boca Raton: Taylor & Francis: 2023).
28. D. A. Lesyk, B. N. Mordyuk, K. E. Grinkevych, O. O. Pedash, and A. Lamikiz, *Advances in Design, Simulation and Manufacturing VIII. Lect. Notes Mech. Eng.* (Eds. V. Ivanov *et al.*) (Cham: Springer: 2025).
29. D. A. Lesyk, S. Martinez, B. N. Mordyuk, D. Grochala, and A. Lamikiz, *New Technologies, Development and Application VII. Lect. Notes Networks Syst.* (Eds. I. Karabegović *et al.*) (Cham: Springer: 2024), vol. **1069**, p. 201.
30. H. Zou, J. Ying, X. Ma, Y. Chen, B. Han, and J. Zhan, *Surf. Sci. Technol.*, **2**, No. 17: 46 (2024).
31. J. Guo, K. H. Au, C.-N. Sun, M. H. Goh, C. W. Kum, K. Liu, J. Wei, H. Suzuki, and R. Kang, *J. Mater. Process. Technol.*, **264**: 422 (2019).
32. M. Marczak, D. A. Moszczynska, and A. P. Wawrzyszcz, *Appl. Sci.*, **15**, Iss. 15: 8233 (2025).
33. Y. Zhao, J. Ratay, K. Li, H. Yamaguchi, and W. Xiong, *J. Manuf. Mater. Process.*, **6**, Iss. 2: 43 (2022).
34. L. Emanuelli, F. Deirmina, and M. Pellizzari, *Mater. Charact.*, **199**: 112788 (2023).
35. W. Tillmann, C. Schaak, J. Nellesen, M. Schaper, M. E. Aydinöz, and K.-P. Hoyer, *Addit. Manuf.*, **13**: 93 (2017).
36. D. A. Lesyk, S. Martinez, O. O. Pedash, V. V. Dzhemelinskyi, and A. Lamikiz, *MRS Adv.*, **7**: 197 (2022).
37. X. Xu, Q. Shen, B. Han, J. Tang, J. Ying, and H. Yang, *J. Magn. Magn. Mater.*, **630**: 173458 (2025).
38. G. Liu, H. Yang, X. Xu, and B. Han, *JMMM*, **655**: 174353 (2026).
39. Y. Kaynak and E. Tascioglu, *Prog. Addit. Manuf.*, **5**: 221 (2020).
40. M. Ham, S. Park, H. Lee, D. H. Kim, J. H. Sung, G. K. Ahn, G. S. Kim, and B. Lee, *J. Manuf. Process.*, **156A**: 569 (2025).
41. M. Khorasani, A. H. Ghasemi, E. Farabi, M. Leary, I. Gibson, and B. Rolfe, *Int. J. Adv. Manuf. Technol.*, **120**: 3471 (2022).